

폴리프로필렌/폴리아미드 엘라스토머 블렌드: 모폴로지와 기계적 물성

Qingsheng Liu[†], Yan Xu, Hongxia Zhang*, Yuhao Li**, and Bingyao Deng[†]

Key Laboratory of Eco-Textiles (Ministry of Education), Jiangnan University

*Wuxi Entry-Exit Inspection and Quarantine Bureau, **China Nonwovens & Industrial Textiles Association

(2014년 2월 10일 접수, 2014년 4월 15일 수정, 2014년 4월 22일 채택)

Polypropylene/Polyamide Elastomer Blends: Morphology and Mechanical Property

Qingsheng Liu[†], Yan Xu, Hongxia Zhang*, Yuhao Li**, and Bingyao Deng[†]

Key Laboratory of Eco-Textiles (Ministry of Education), Jiangnan University, Wuxi 214122, China

*Wuxi Entry-Exit Inspection and Quarantine Bureau, Wuxi 214101, China

**China Nonwovens & Industrial Textiles Association, Beijing 100742, China

(Received February 10, 2014; Revised April 15, 2014; Accepted April 22, 2014)

Abstract: The polypropylene/polyamide elastomer (PP/PAE) blends were prepared by melt mixing. PP and PAE in PP/PAE were immiscible completely. The size of PAE domains was large and the clear gap in the interface between PP and PAE existed, which did not meet the conditions enhancing toughness of polymers by elastomer. Therefore, maleic anhydride grafted polypropylene (MP) was used to improve the miscibility between PP and PAE. The miscibility between PP and PAE was improved and the size of dispersed phase PAE decreased by introducing MP. The crystallization of PP became easier by introducing PAE as a nucleating agent. With the increase of PAE content, the melt-crystallization temperatures of PP components in PP/PAE/MP blends increased gradually. The melt-crystallization of the polytetramethylene oxide segment of PAE component in PP/PAE blends were hampered by PP component. In addition, PAE can enhance significantly the toughness of PP, and the tensile strength and modulus did not decrease.

Keywords: polypropylene, polyamide elastomer, morphology, crystallization, mechanical property.

Introduction

Polypropylene (PP) is quite an outstanding polymeric material with respect to its performance, in particular its wide property spectrum, easy processability, versatility of applications and attractive combination of favorable economics.^{1,2} However, its toughness is not sufficient for the application as engineering plastic.^{3,4} Toughening polymers by using elastomer is one of the most widely used methods.^{5,6} For instance, poly(styrene-ethylene-butylene-styrene) (SEBS),⁷ ethylene-propylene rubber (EPR),⁷ ethylene-propylene-diene monomer elastomer (EPDM),⁷ ethylene-hexene rubber,⁷ ethylene-octene copolymer (EOC),⁸ polyisobutylene (PIB)⁸ and styrene-butadiene block copolymer (SBS)⁸ and so on have been used to improve its toughness. Generally speaking, the improvement of toughness of PP by using elastomer is at the expense of its mechan-

ical strength and stiffness.⁹ However, Zhang *et al.*¹⁰ found that when a small amount of poly(ether-*block*-amide) elastomer (PAE) (5 wt%) was added to polylactide (PLA), the elongation at break of PLA/PAE blend could reach 161.5% while the tensile strength was 48.1 MPa, which was a bit larger than that of neat PLA. It is possible that the PAE would enhance toughness of PP at no expense of its mechanical strength and stiffness. The toughened PP can be widely used as household appliance, medical ware, automotive, construction and other industrial sections.⁹ It is well known that the miscibility between PP and elastomer as well as phase morphology of the PP blends play the dominant role in determining the effectiveness of the elastomers on impact enhancement. In addition, good adhesion between the dispersed elastomer particle and PP matrix is essential to achieve effective impact enhancement.¹¹ Therefore, in this paper, PAE was chosen to enhance toughness of PP. Maleic anhydride grafted polypropylene (MP) as a compatible agent was used to improve the miscibility between PP and PAE. The morphology, crystallization behavior, and mechan-

[†]To whom correspondence should be addressed.
E-mail: qslu@jiangnan.edu.cn; bydeng@jiangnan.edu.cn

ical property of PP/PAE blends were studied in details by SEM, DSC and Instron 3385H tensile strength test machine.

Experimental

Material Preparation. PP with melt flow rate (MFR) of 30 g/10 min was purchased from Zhejiang Guangyuan Petrochemical Co., Ltd. (China). The polyamide elastomer (PAE) was supplied by Atofina Chemicals Corporation (France), which was named PEBAX 2533 commercially. PEBAX2533 is a kind of block copolymer [poly(ether-*block*-amide)] containing polytetramethylene oxide (PTMO) and polyamide 12 (PA12) units. The weight percent of the PTMO blocks with the weight-average molecular weight (M_w) of 2000 is 78% and that of the PA blocks (PA12) with the M_w of 530 is 22%. Maleic anhydride grafted polypropylene (MP) was purchased from Nanjing Deba Chemical Co., Ltd..

The PP, PAE and MP were dried at 65 °C for 48 h in vacuum oven before processing. The blends were prepared by melt mixing in a SJSZ-10A twin-screw microcompounder (Wuhan Rayzone Ming Plastics Machinery Co., Ltd.). Polymers were mixed at screw speed of 20 rpm for 5 min at 190 °C. In addition, the neat PP was subjected to the same mixing treatment so that neat PP had the same thermal history as the blends. The compositions of blends were presented in Table 1.

Table 1. Compositions of Blends

| No. | Name | PP (wt%) | PAE (wt%) | MP (wt%) |
|-----|---------|----------|-----------|----------|
| 1 | 100/0/0 | 100 | 0 | 0 |
| 2 | 0/100/0 | 0 | 100 | 0 |
| 3 | 0/0/100 | 0 | 0 | 100 |
| 4 | 80/20/0 | 80 | 20 | 0 |
| 5 | 77/20/3 | 77 | 20 | 3 |
| 6 | 89/10/1 | 89 | 10 | 1 |
| 7 | 88/10/2 | 88 | 10 | 2 |
| 8 | 87/10/3 | 87 | 10 | 3 |
| 9 | 86/10/4 | 86 | 10 | 4 |
| 10 | 85/10/5 | 85 | 10 | 5 |
| 11 | 84/10/6 | 84 | 10 | 6 |
| 12 | 91/5/4 | 91 | 5 | 4 |
| 13 | 76/20/4 | 76 | 20 | 4 |
| 14 | 66/30/4 | 66 | 30 | 4 |
| 15 | 0/80/20 | 0 | 80 | 20 |

Scanning Electron Microscope. Scanning electron microscope (SEM) measurements were carried out with a Model S-4800 field emission scanning electron microscope (Hitachi, Japan). The samples were broken into pieces in liquid nitrogen, and then were sputtered with gold. The morphologies of cross section of samples were observed under a working voltage of 10 kV.

Fourier Transform Infrared Attenuated Total Reflection Spectroscopy. Spectra of Fourier transform infrared attenuated total reflection (FTIR-ATR) were recorded on a Nicolet FTIR spectroscope (Nexus 670). Each spectrum was recorded with a total of 16 scans; each had a resolution of 4 cm⁻¹ at room temperature. Software of OMNIC Nicolet was used for spectra analysis.

Differential Scanning Calorimetry. The crystallization behaviors and melting behaviors of samples were characterized by differential scanning calorimetry (DSC) that used a DSC Q200 (TA Instruments®, Inc.). Nitrogen was used at a flow rate of 50 mL/min. The instrument was calibrated with In and Pb. The weight of the samples was in the range of 4–6 mg.

Measurements of Tensile Properties. Tensile properties were determined on Instron 3385H tensile strength test machine using dumb-bell specimens at room temperature. The dumb-bell specimens were prepared by injection molding at 190 °C, 5 MPa for 3 min on a SZ-15 injection-molding machine (Wuhan Rayzone Ming Plastics Machinery Co., Ltd.). The cross-head speed and gauge length of the apparatus were 50 mm/min and 50 mm, respectively.

Results and Discussion

Morphology. Figure 1 represented the SEM photos of the PP/PAE blend with 20 wt% PAE. Figure 1(a) showed that PAE with the dimension of ca. 10 μm was dispersed in PP matrix uniformly. The part in the white frame in Figure 1(a) was enlarged in Figure 1(b). Figure 1(b) showed clearly that the shape of the PAE domains in the PP matrix was spherical, the fractured interface was smooth, some PAE particles were protruberant, the interface between PP and PAE was clear, and the gap could be observed, which illustrated that PP and PAE was immiscible completely. It was reported that some conditions should be met to improve the toughness of brittle polymer by using elastomers.^{12,13} Firstly, the elastomer must be distributed as small domains in the polymer matrix. Secondly, the elastomer must have good interfacial adhesion to the polymer. Thirdly, the rubber should not be miscible with matrix poly-

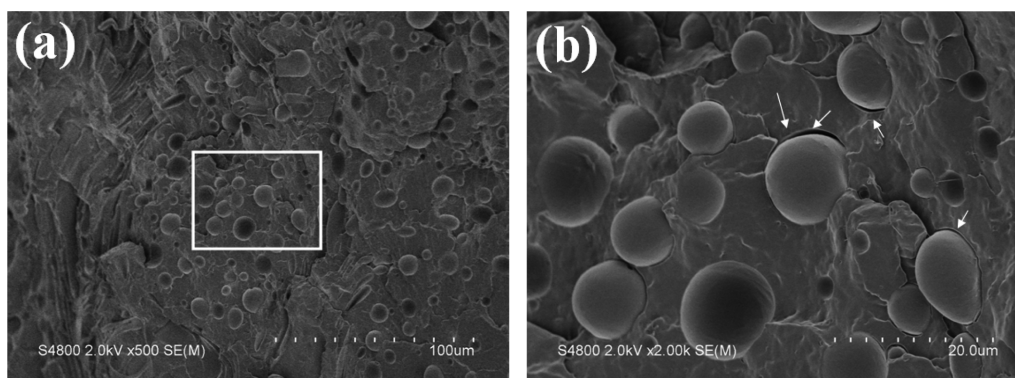


Figure 1. SEM micrographs of the PP/PAE blend with 20 wt% PAE.

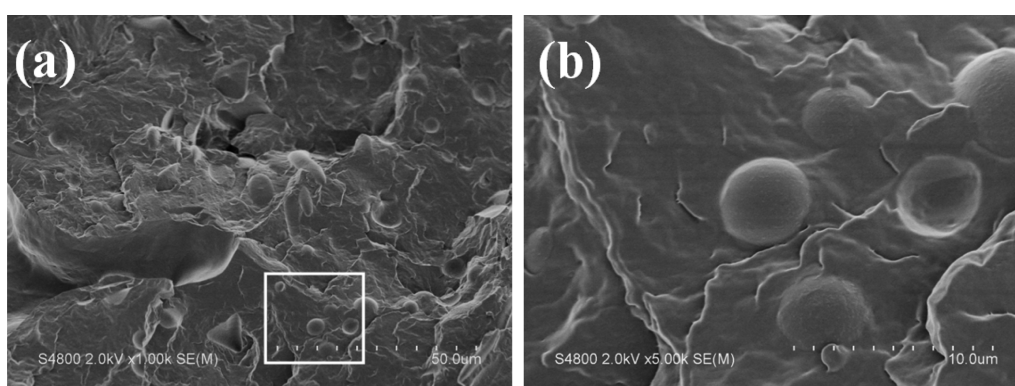


Figure 2. SEM micrographs of the PP/PAE/MP (77/20/3) blend.

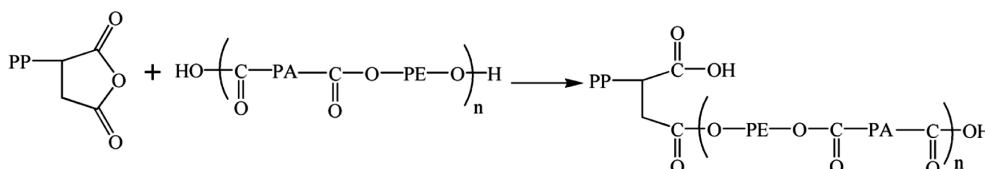


Figure 3. Scheme of reaction between PAE and MP.

mer. Here, the dispersed phase was large. The interfacial adhesion between PP and PAE was poor. Therefore, it was inferred that the toughness of PP could not be improved by addition of PAE. It is well known that compatibilizer can reduce the size of dispersed phases and enhance the interfacial adhesion. Thus, MP was selected as the compatibilizer to add the PP/PAE blends to alter the structure of blends and improve the properties of blends.

3 wt% MP was added to PP/PAE blend with 20 wt% PAE. The SEM photos of PP/PAE/MP blend (77/20/3) were shown in Figure 2. The PAE phases were dispersed uniformly in PP matrix. Compared with PP/PAE without MP, the size of PAE in PP/PAE with MP which was ca. 5 μm decreased obviously. In addition, the interface between PP and PAE was obscure,

which indicated that the interaction between PP and PAE existed by the bridge of MP. The reason was as follows. The maleic anhydride in MP could react with hydroxyl groups in PAE at the PP/PAE interface, and this led to the formation of a graft copolymer (Figure 3), which reduced the interfacial tension and improved the compatibility between PP and PAE.

Figure 4 illustrated FTIR spectra of neat PAE (0/100/0), neat MP (0/0/100), and PAE/MP blend (0/80/20). In FTIR spectrum of neat MP, the peak at 1704 cm^{-1} was attributed to anhydride groups of MP.¹⁴ However, in FTIR spectrum of PAE/MP blend, the peak at 1704 cm^{-1} was not observed, which showed that the reaction between MP and PAE happened.

PP/PAE blends with 10 wt% PAE were chosen to study the effect of compatibilizer on morphology of PP/PAE blends by

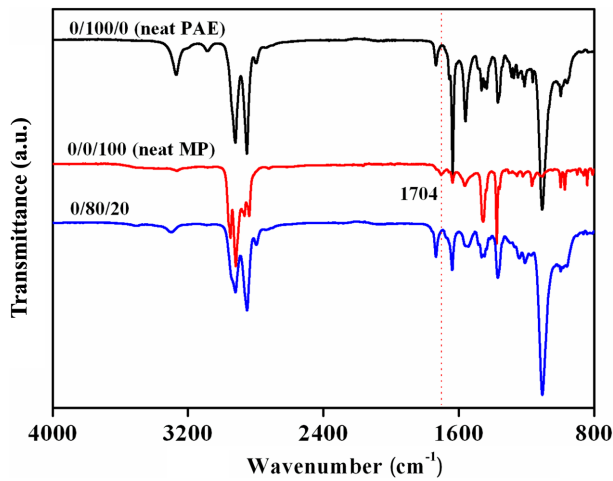


Figure 4. FTIR spectra of neat PAE (0/100/0), neat MP (0/0/100), and PAE/MP blend (0/80/20).

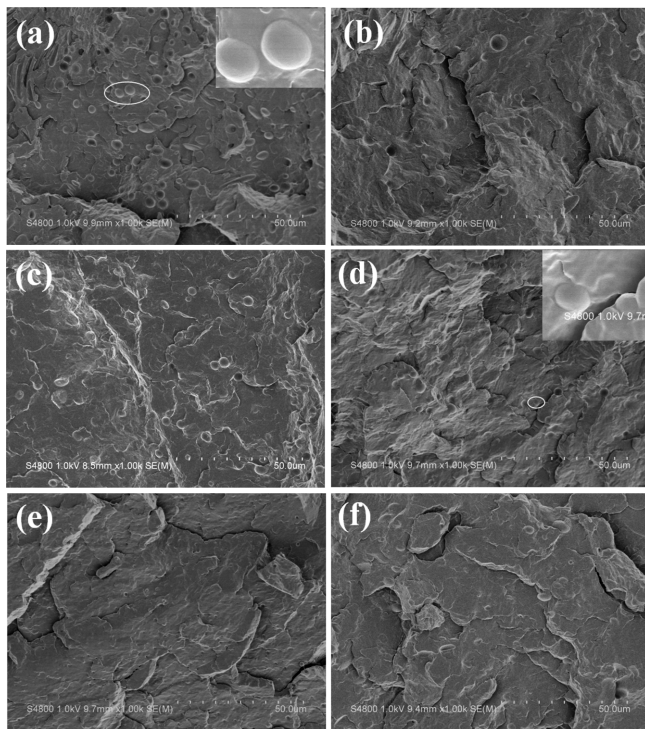


Figure 5. SEM micrographs of the PP/PAE/MP blends: (a) 89/10/1; (b) 88/10/2; (c) 87/10/3; (d) 86/10/4; (e) 85/10/5; (f) 84/10/6.

altering the MP content. The SEM photos of the PP/PAE blend with 10 wt% PAE and different MP content were shown in Figure 5. Figure 5(a) showed that when the MP content was 1 wt%, the size of PAE domains was ca. 5 μm . It can be seen from Figure 5(a)–(d) that with the increase of MP content below 4 wt%, the size of PAE domains decreased gradually. When the MP content was 4 wt%, the size of PAE domains was ca. 3 μm , which was illustrated in Figure 5(d). With the

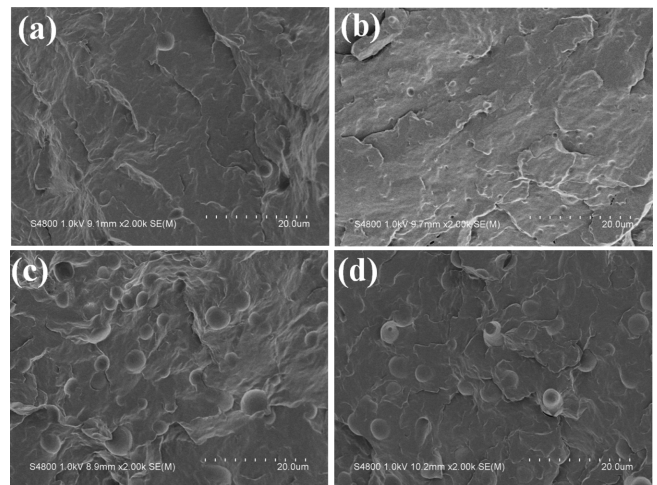


Figure 6. SEM micrographs of the PP/PAE/MP blends: (a) 91/5/4; (b) 86/10/4; (c) 76/20/4; (d) 66/30/4.

further increase of MP content above 4 wt%, the size of PAE almost did not change. The parts located in white circle in Figure 5(a) and (d) were enlarged, which was showed in the upper right corner of Figure 5(a) and (d), respectively so that the morphologies of blends could be observed clearly. It can be seen that the interface between PAE and PP in blends with 4 wt% MP was more obscure than the one in blends with 1 wt% MP, which showed that the more intense interfacial adhesion existed in PP/PAE blends with 4 wt% MP.

The MP was fixed at 4 wt% by altering the content of PAE so that the effect of PAE content on the morphologies of PP/PAE blends was investigated. The SEM photos of PP/PAE/MP blends with different PAE content were shown in Figure 6. Figure 6 illustrated that for a PP/PAE/MP blend, the PAE domains were dispersed uniformly in PP matrix and the interface between PP and PAE was obscure. In addition, with the increase of PAE content from 5–30 wt%, the size of PAE domains increased gradually from 3 to 6 μm .

Crystallization and Melting Behavior of PP/PAE/MP. The nonisothermal crystallization and melting behavior of PP/PAE/MP blends were investigated by DSC. Figure 7(a) showed the cooling DSC curves of PP/PAE/MP blends and neat PP from the melt to $-90\text{ }^{\circ}\text{C}$ at $10\text{ }^{\circ}\text{C}/\text{min}$. In the cooling DSC curves of neat PP, only single melt-crystallization peak appeared at $114.8\text{ }^{\circ}\text{C}$. However, for a PP/PAE/MP blend, two melt-crystallization peaks were observed. The temperatures in the high temperatures were attributed to the melt-crystallization temperature ($T_{\text{mc}}(\text{PP})$) of PP component while the ones in the low temperature range were attributed to the melt-crystallization one ($T_{\text{mc}}(\text{PTMO})$) of PTMO segment of PAE. In

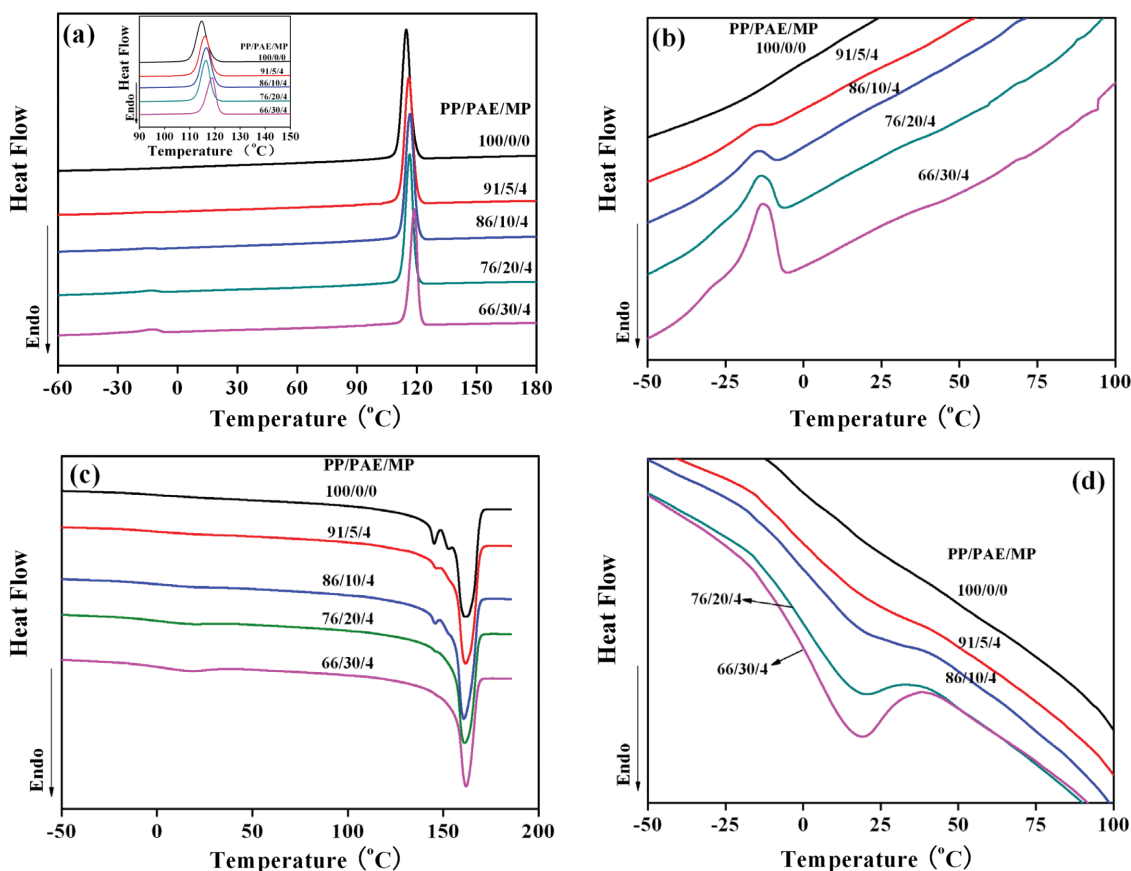


Figure 7. DSC curves of PP/PAE/MP blends and neat PP: (a) cooling process at 10 °C/min; (b) the low temperature districts corresponding to the melt-crystallization of PTMO segment of PAE components in (a); (c) the second heating process at 10 °C/min; (d) the districts corresponding to melting of PTMO segment of PAE component in (c).

Table 2. Nonisothermal Crystallization and Melting Parameters of PP/PAE/MP Blends and Neat PP

| PP/PAE/MP | $T_{mc}(\text{PTMO})$ (°C) | $T_{mc}(\text{PP})$ (°C) | $T_m(\text{PTMO})$ (°C) | $\Delta H_m(\text{PTMO})$ (J/g) | $T_m(\text{PP})$ (°C) |
|-----------|----------------------------|--------------------------|-------------------------|---------------------------------|-----------------------|
| 100/0/0 | – | 114.8 | – | – | 162.4 |
| 91/5/4 | -16.0 | 116.1 | 15.5 | 1.66 | 161.8 |
| 86/10/4 | -15.3 | 116.6 | 17.7 | 2.55 | 160.9 |
| 76/20/4 | -14.2 | 116.4 | 15.6 | 4.28 | 161.2 |
| 66/30/4 | -13.4 | 118.8 | 16.8 | 7.21 | 162.0 |

Figure 7(a), it was difficult to observe the melt-crystallization peaks of PTMO segment of PAE components. In order to observe clearly the melt-crystallization peaks of PTMO segment of PAE components, the low temperature districts corresponding to the melt-crystallization of PTMO segment of PAE components were illustrated in Figure 7(b). The values of $T_{mc}(\text{PP})$ and $T_{mc}(\text{PTMO})$ were listed in Table 2. It was reported by our previous literature¹³ that $T_{mc}(\text{PTMO})$ in neat PAE was -11.7°C. $T_{mc}(\text{PTMO})$ of neat PAE was higher than $T_{mc}(\text{PTMO})$ s of blends, which showed that melt-crystallization of the PTMO

segment of PAE component in PP/PAE blends were hampered by PP component. It could be seen from Figure 7(b) and Table 2 that with the increase of PAE in PP/PAE/MP, the $T_{mc}(\text{PTMO})$ s increased gradually, due to the decrease of PP content. Figure 7(b) and Table 2 also illustrated that $T_{mc}(\text{PP})$ of neat PP was lower than those of PP components in PP/PAE/MP blends, which showed that the crystallization of PP became easier by introducing PAE as a nucleating agent. In addition, with the increase of PAE content, $T_{mc}(\text{PP})$ of PP components in PP/PAE/MP blends increased gradually. Figure 7(c) showed the

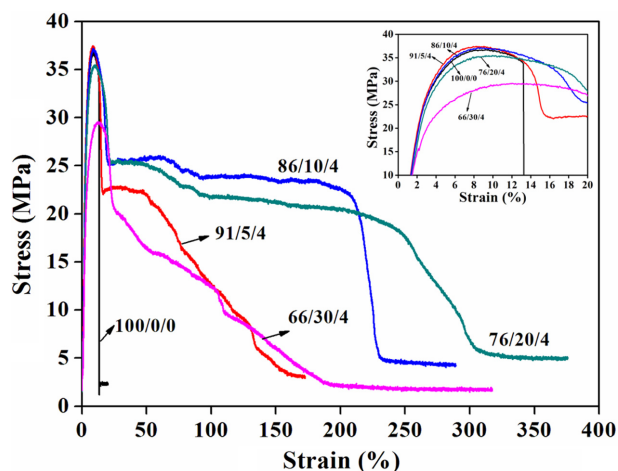


Figure 8. Stress-strain curves of PP/PAE/MP blends and neat PP.

second heating DSC curves of PP/PAE/MP blends and corresponding neat PP at 10 °C/min. In the heating DSC curves of neat PP, only a melting peak was observed at 162.4°C. In the heating DSC curves of PP/PAE/MP blends, the endothermic peaks at low temperature part were attributed to melting of PTMO segment of PAE component, which were too weak to be observed. The districts corresponding to melting of PTMO segment of PAE component were shown in Figure 7(d) so that they could be observed clearly. The endothermic peaks of PP/PAE/MP blends at high temperature part were mainly attributed to melting of PP component. The data of T_m (PTMO), ΔH_m (PTMO) and T_m (PP) were also listed in Table 2. It could be seen from Table 2 that the values of ΔH_m (PTMO) were so small that it was difficult to observe clearly the melting peaks of PTMO segments of PAE in PP/PAE/MP blends. In addition, with the increase of PAE content, the values of ΔH_m (PTMO) increased gradually. Figure 7(c) and Table 1 also showed that T_m (PP) did not almost change.

Mechanical Property. Figure 8 presented stress-strain curves of PP/PAE/MP blends and neat PP. Figure 8 illustrated that the yield stress of neat PP was 36.7 MPa, and elongation at break was 13.3%, which was small. This showed that neat PP was brittle. However, for all the blends, the toughness increased in comparison with neat PP. With the increase of PAE, the toughness increased gradually. When PAE content was 20 wt%, elongation at break reached maximum of more than 300%. When PAE content was above 30%, the toughness decreased. In addition, it was surprising that when PAE content was 10 wt%, the elongation at break of the blend was beyond 200%, and the yield stress and the initial modulus of the blend was a bit larger than those of neat PP.

Conclusions

The polypropylene/polyamide elastomer (PP/PAE) blends were prepared by melt mixing using two-screw extruder. PP and PAE in PP/PAE were immiscible completely. For PP/PAE blend with 20 wt% PAE, the size of PAE domains was ca. 10 μm . which was large. In addition, the interfacial adhesion between PP and PAE was poor, which did not meet the conditions enhancing toughness of polymers by elastomer. In order to reduce the size of dispersed phase and improve the miscibility between PP and PAE, MP were introduced to PP/PAE blends. For PP/PAE with 10 wt%, with the increase of MP content below 4 wt%, the size of PAE domains decreased gradually. With the further increase of MP content above 4 wt%, morphology of PAE almost did not change. In addition, the effect of PAE content on crystallization behavior and mechanical property of PP/PAE/MP with 4 wt% MP has been studied. The results showed that the crystallization of PP became easier by introducing PAE as a nucleating agent. With the increase of PAE content, the melt-crystallization temperatures of PP components in PP/PAE/MP blends increased gradually. In addition, PAE could enhance significantly the toughness of PP, and the tensile strength and modulus did not decrease.

Acknowledgements: This work was supported by the Natural Science Foundation of Jiangsu Province (No.BK20130142), the Open Project Program of Key Laboratory of Advanced Textile Materials and Manufacturing Technology (Zhejiang Sci-Tech University), Ministry of Education (No.2013004), the Open Project Program of State Key Laboratory for Modification of Chemical Fibers and Polymer Materials, Dong Hua University (No. LK1216), the Public Technology Applied Research Projects of Science Technology Bureau of Shaoxing (No. 2012B70009), and the Industrial Support Program of Suqian (H201313).

References

1. M. Denac, I. Šmit, and V. Musil, *Compos. Part A: Appl. Sci. Manuf.*, **36**, 1094 (2005).
2. M. Denac, V. Musil, and I. Šmit, *Compos. Part A: Appl. Sci. Manuf.*, **36**, 1282 (2005).
3. J. H. Park, Y.-T. Sung, W. N. Kim, J. H. Hong, B. K. Hong, T. W. Yoo, and H. G. Yoon, *Polymer(Korea)*, **29**, 19 (2005).
4. K.-H. Seo and J.-C. Lim, *Polymer(Korea)*, **25**, 707 (2001).
5. M. L. Q. A. Kaneko, R. B. Romero, R. E. F. D. Paiva, M. I.

- Felisberti, M. C. Goncalves, and I. V. P. Yoshida, *Polym. Compos.*, **34**, 194 (2013).
6. L. Zhang, R. Huang, G. Wang, L. Li, H. Ni, and X. Zhang, *J. Appl. Polym. Sci.*, **86**, 2085 (2002).
7. R. Keskin and S. Adanur, *Polym.-Plast. Technol. Eng.*, **50**, 20 (2011).
8. M. Ichazo, M. Hernández, J. González, C. Albano, and N. Domínguez, *Polym. Bull.*, **51**, 419 (2004).
9. S. P. Bao and S. C. Tjong, *Compos. Part A: Appl. Sci. Manuf.*, **38**, 378 (2007).
10. W. Zhang, L. Chen, and Y. Zhang, *Polymer*, **50**, 1311 (2009).
11. R. Zhao and G. Dai, *J. Appl. Polym. Sci.*, **86**, 2486 (2002).
12. N. Bitinis, R. Verdejo, P. Cassagnau, and M. A. Lopez-Manchado, *Mater. Chem. Phys.*, **129**, 823 (2011).
13. Q. Liu, H. Zhang, M. Zhu, Z. Dong, C. Wu, J. Jiang, X. Li, F. Luo, Y. Gao, B. Deng, Y. Zhang, J. Xing, H. Wang, and X. Li, *Fiber. Polym.*, **14**, 1688 (2013).
14. E. S. Ogunniran, R. Sadiku, S. S. Ray, and N. Luruli, *Macromol. Mater. Eng.*, **297**, 627 (2012).